

# Lecture 7: Deformable mirror modeling and control

Rufus Fraanje  
`p.r.fraanje@tudelft.nl`

TU Delft — Delft Center for Systems and Control

Jun. 20, 2011

# Outline

- 1 Adjustable optics in nature and engineering;
- 2 Deformable mirrors — modeling;
- 3 Control of AO systems;
- 4 Exams

# Outline

- 1 Adjustable optics in nature and engineering;
- 2 Deformable mirrors — modeling;
- 3 Control of AO systems;
- 4 Exams

# Outline

- 1 Adjustable optics in nature and engineering;
- 2 Deformable mirrors — modeling;
- 3 Control of AO systems;
- 4 Exams

# Outline

- 1 Adjustable optics in nature and engineering;
- 2 Deformable mirrors — modeling;
- 3 Control of AO systems;
- 4 Exams

# Adjustable optics

- 1 Adjustable pupils (size/shape);
- 2 Adjustable lenses (focus);
- 3 Adjustable pointing direction (tip/tilt);
- 4 Deformable mirrors.

# Adjustable optics

- 1 Adjustable pupils (size/shape);
- 2 Adjustable lenses (focus);
- 3 Adjustable pointing direction (tip/tilt);
- 4 Deformable mirrors.

# Adjustable optics

- 1 Adjustable pupils (size/shape);
- 2 Adjustable lenses (focus);
- 3 Adjustable pointing direction (tip/tilt);
- 4 Deformable mirrors.



# Adjustable optics

- 1 Adjustable pupils (size/shape);
- 2 Adjustable lenses (focus);
- 3 Adjustable pointing direction (tip/tilt);
- 4 Deformable mirrors.

# Adjustable optics — Nature

Adjustable pupils (from: Animal Eyes, Land&Nilsson, 2002)

Lens eyes on land 89 |

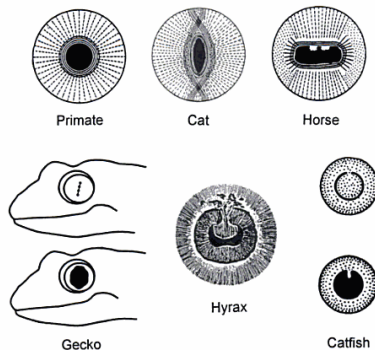


**Fig. 5.11** Pupil shapes in vertebrates. *Top row:* round and slit-shaped pupils in mammals, showing how the cat's slit pupil can close further than the circular primate pupil. Iris closer muscles are continuous lines and opener muscles dashed lines. *Bottom row:* gecko pupil contracts to four 'pin-holes' in the light. The hyrax or coney (*Procavia*, a small desert mammal) has a pupil partly closed by a central operculum, which acts as a sunshade. A similar mobile operculum is present in some fish, such as the catfish *Plecostomus*. Combined from Walls (1941).

# Adjustable optics — Engineering

Adjustable pupils: (Source: Wikipedia)



“Minolta” lens,  $f/1.5 - f/16$

Numerical aperture (NA):

$$NA = \frac{f}{D} \quad f/NA = D$$

NA of E-ELT: 17.7, NA of human eye?

# Adjustable optics — Engineering

Adjustable pupils: (Source: Wikipedia)



“Minolta” lens,  $f/1.5 - f/16$

$f/32$  (top-left) and  $f/5$  (bottom-right)

Numerical aperture (NA):

$$NA = \frac{f}{D} \quad f/NA = D$$

NA of E-ELT: 17.7, NA of human eye?

# Adjustable optics — Engineering

Adjustable pupils: (Source: Wikipedia)



“Minolta” lens,  $f/1.5 - f/16$

$f/32$  (top-left) and  $f/5$  (bottom-right)

Numerical aperture (NA):

$$NA = \frac{f}{D} \quad f/NA = D$$

NA of E-ELT: 17.7, NA of human eye?

# Adjustable optics — Engineering

Adjustable pupils: (Source: Wikipedia)



“Minolta” lens,  $f/1.5 - f/16$

$f/32$  (top-left) and  $f/5$  (bottom-right)

Numerical aperture (NA):

$$NA = \frac{f}{D} \quad f/NA = D$$

NA of E-ELT: 17.7, NA of human eye?

# Adjustable optics — Engineering

Adjustable pupils: (Source: Wikipedia)



“Minolta” lens,  $f/1.5 - f/16$

$f/32$  (top-left) and  $f/5$  (bottom-right)

Numerical aperture (NA):

$$\text{NA} = \frac{f}{D} \quad f/\text{NA} = D$$

NA of E-ELT: 17.7, NA of human eye? Answer:  $\approx \frac{1.7}{0.7} = 2.4$

# Adjustable optics — Nature

## Adjustable lenses (from: Animal Eyes, Land&Nilsson, 2002)

Lens eyes on land 83

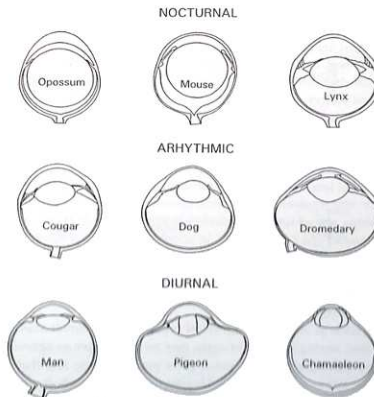


**Fig. 5.7** Variations in the structure of eyes from animals with different terrestrial lifestyles (not on the same scale). Nocturnal animals have the biggest lenses and diurnal animals the smallest; animals active day and night (arhythmic) have intermediate eyes. Adapted from Walls (1941).



# Adjustable optics — Engineering

Adjustable lenses (Source: <http://www.nedinsco.nl>):

Day Sight TV Camera VZC-RZ230 MSP

**Application** Searching

## Characteristics

Detector	1/2" CCD monochrome
Optics	Continuous Zoom max. 10x
Focus Range	$\leq 10\text{m} - \infty$
Dynamic Range	1 to 150.000 Lux
Wavelength	400 to 1000 nm
Field of View Horizontal	$\leq 2,5^\circ$ to $\leq 24^\circ$

## Mechanical

Dimensions	245 x 139 x 111 mm
Weight	2,3 kg

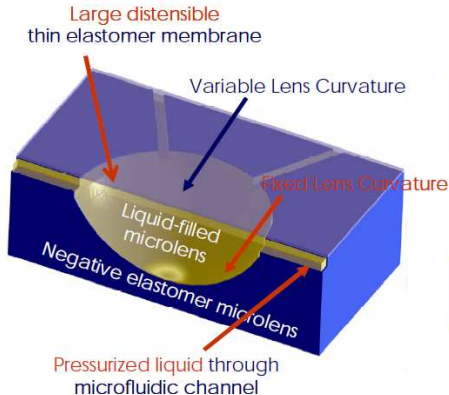
## Environmental

Complies with	MIL-STD 810 & 461
MTBF	$\geq 10.000\text{ h}$



# Adjustable optics — Engineering

Adjustable lenses (Source: Jeong et al. (2005), c.f. <http://biopoems.berkeley.edu>)



Biconvex

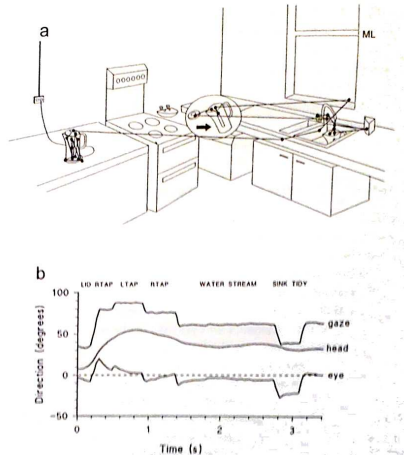


Meniscus

# Adjustable optics — Nature

## Eye/head movement (from: Animal Eyes, Land&Nilsson, 2002)

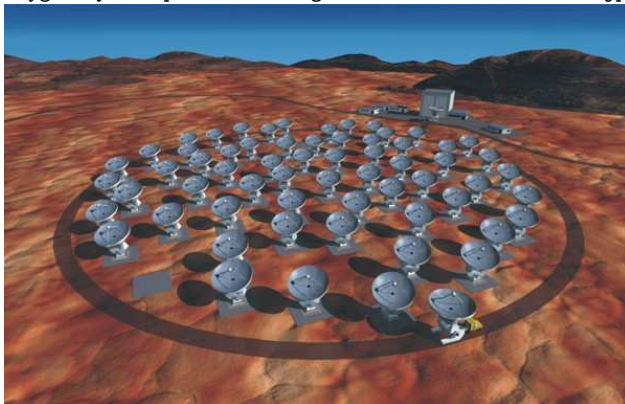
180 Animal Eyes



# Adjustable optics — Engineering

Telescope pointing (Source:

[http://www.dailygalaxy.com/photos/uncategorized/2007/08/12/alma\\_2.jpg](http://www.dailygalaxy.com/photos/uncategorized/2007/08/12/alma_2.jpg)):



ALMA: Atacama Large Millimeter Array (66 telescopes when completed)

# Adjustable optics — Nature

Mirrors in scallops (from: Animal Eyes, Land&Nilsson, 2002)

Mirrors in animals 107

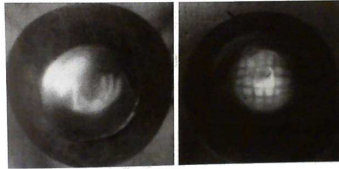


Fig. 6.3 Images in scallops' eyes. *Left*: self-portrait of the author, whose hand is holding the microscope objective used to photograph the eye. *Right*: a grid of 3 mm squares, 15 mm from the eye.



(Source: Wikipedia – Sint-Jakobsschelp)

# Adjustable optics — Engineering

Adjustable mirrors (Keck II, Source: Wikipedia):



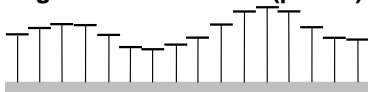
# Adjustable optics — Engineering

Adjustable mirrors (Electrostatic deformable mirror, Source: Flexible Optical, BV, Rijswijk):



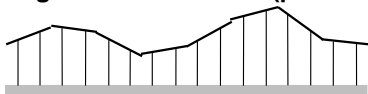
# Deformable mirrors

- **Segmented facesheet (piston):**



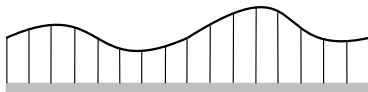
Liquid Crystals, DLP's  
very high actuator density

- **Segmented facesheet (piston/tip/tilt):**



very large (M1's) or MEMS devices  
high actuator density

- **Continuous facesheet:**



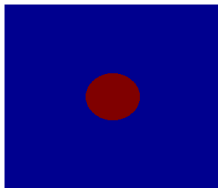
various types (electrostatic, reluctance,  
piezo, ...)  
medium sized diameters (cm range)  
'no' photon loss, low spatial aliasing



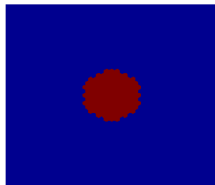
# Deformable mirrors

## Diffraction effects of hexagonal segmented mirrors: Apertures:

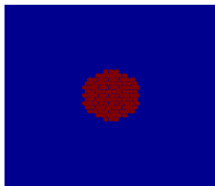
Circular aperture



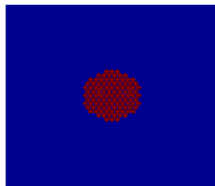
Hexagonal aperture (100% fill)



Hexagonal aperture (95% fill)



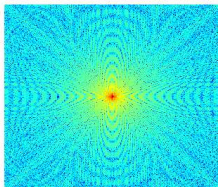
Hexagonal aperture (90% fill)



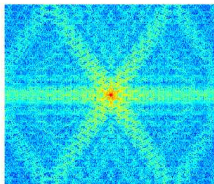
# Deformable mirrors

## Diffraction effects of hexagonal segmented mirrors: Point spread functions:

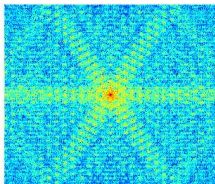
Circular aperture



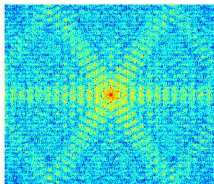
Hexagonal aperture (100% fill)



Hexagonal aperture (95% fill)



Hexagonal aperture (90% fill)



# Deformable mirrors

**Diffraction effects of hexagonal segmented mirrors:**      Obtained images:

Circular aperture



Hexagonal aperture (100% fill)



Hexagonal aperture (90% fill)

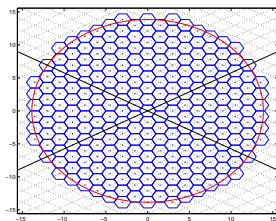
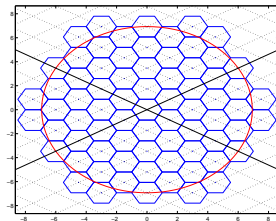
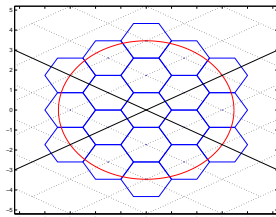
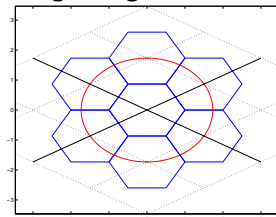


Hexagonal aperture (70% fill)



# Deformable mirrors

## Hexagonal grids



6 corner points:

$$\begin{bmatrix} \pm 1 \\ 0 \end{bmatrix}, \begin{bmatrix} \pm \frac{1}{2} \\ \pm \frac{\sqrt{3}}{2} \end{bmatrix}$$

hex- to rect.-coord.:

$$\begin{bmatrix} x_r \\ y_r \end{bmatrix} = \begin{bmatrix} \frac{3}{2} & \frac{3}{2} \\ -\frac{\sqrt{3}}{2} & \frac{\sqrt{3}}{2} \end{bmatrix} \begin{bmatrix} x_h \\ y_h \end{bmatrix}$$

rotationally-symmetric over  
 $60^\circ$  angles.

# Deformable mirrors — modeling

Let  $w(x, y, t)$  be the out-of-plane deformation and  $p(x, y, t)$  the distributed pressure from, e.g., actuators.

- **Membrane mirror:**

$$\left(\frac{1}{c^2} \frac{\partial^2}{\partial t^2} - \nabla^2\right) w(x, y, t) = p(x, y, t)$$

+boundary/initial conditions, where  $\nabla^2 = \partial^2/\partial x^2 + \partial^2/\partial y^2$

- **Thin plate mirror:**

$$\left(\rho h \frac{\partial^2}{\partial t^2} + E/\nabla^4\right) w(x, y, t) = p(x, y, t)$$

+boundary/initial conditions, where  $\nabla^4 = \partial^4/\partial x^4 + 2\partial^4/\partial x^2\partial y^2 + \partial^4/\partial y^4$ .

c.f. Timoshenko et al., *Theory of Plates and Shells*, McGraw-Hill, 1959.

# Deformable mirrors — modeling

Let  $w(x, y, t)$  be the out-of-plane deformation and  $p(x, y, t)$  the distributed pressure from, e.g., actuators.

- **Membrane mirror:**

$$\left(\frac{1}{c^2} \frac{\partial^2}{\partial t^2} - \nabla^2\right) w(x, y, t) = p(x, y, t)$$

+boundary/initial conditions, where  $\nabla^2 = \partial^2/\partial x^2 + \partial^2/\partial y^2$

- **Thin plate mirror:**

$$\left(\rho h \frac{\partial^2}{\partial t^2} + EI \nabla^4\right) w(x, y, t) = p(x, y, t)$$

+boundary/initial conditions, where  $\nabla^4 = \partial^4/\partial x^4 + 2\partial^4/\partial x^2\partial y^2 + \partial^4/\partial y^4$ .

c.f. Timoshenko et al., *Theory of Plates and Shells*, McGraw-Hill, 1959.

# Deformable mirrors — modeling

Solutions obtained by (dynamic or static case):

- finite difference approximation:

$$\left. \frac{\partial w}{\partial x} \right|_{x,y,t} \approx \frac{w(x + \delta x, y, t) - w(x - \delta x, y, t)}{2\delta x}$$

- finite element approximation:

$$w(x, y, t) = \sum_{k=1}^n u_k(t) v_k(x, y), \quad v_k(x, y) \text{ defined over 'finite element'}$$

- modal approximation:

$$w(x, y, t) = \sum_{k=1}^n u_k(t) \phi_k(x, y), \quad \phi_k(x, y) \text{ a solution of homogeneous PDE}$$

- analytical (only for specific forcing functions  $p(x, y, t)$  and boundary conditions), e.g., by separation of variables.

# Deformable mirrors — modeling

Solutions obtained by (dynamic or static case):

- finite difference approximation:

$$\left. \frac{\partial w}{\partial x} \right|_{x,y,t} \approx \frac{w(x + \delta x, y, t) - w(x - \delta x, y, t)}{2\delta x}$$

- finite element approximation:

$$w(x, y, t) = \sum_{k=1}^n u_k(t) v_k(x, y), \quad v_k(x, y) \text{ defined over 'finite element'}$$

- modal approximation:

$$w(x, y, t) = \sum_{k=1}^n u_k(t) \phi_k(x, y), \quad \phi_k(x, y) \text{ a solution of homogeneous PDE}$$

- analytical (only for specific forcing functions  $p(x, y, t)$  and boundary conditions), e.g., by separation of variables.



# Deformable mirrors — modeling

Solutions obtained by (dynamic or static case):

- finite difference approximation:

$$\left. \frac{\partial w}{\partial x} \right|_{x,y,t} \approx \frac{w(x + \delta x, y, t) - w(x - \delta x, y, t)}{2\delta x}$$

- finite element approximation:

$$w(x, y, t) = \sum_{k=1}^n u_k(t) v_k(x, y), \quad v_k(x, y) \text{ defined over 'finite element'}$$

- modal approximation:

$$w(x, y, t) = \sum_{k=1}^n u_k(t) \phi_k(x, y), \quad \phi_k(x, y) \text{ a solution of homogeneous PDE}$$

- analytical (only for specific forcing functions  $p(x, y, t)$  and boundary conditions), e.g., by separation of variables.

# Deformable mirrors — modeling

Solutions obtained by (dynamic or static case):

- finite difference approximation:

$$\left. \frac{\partial w}{\partial x} \right|_{x,y,t} \approx \frac{w(x + \delta x, y, t) - w(x - \delta x, y, t)}{2\delta x}$$

- finite element approximation:

$$w(x, y, t) = \sum_{k=1}^n u_k(t) v_k(x, y), \quad v_k(x, y) \text{ defined over 'finite element'}$$

- modal approximation:

$$w(x, y, t) = \sum_{k=1}^n u_k(t) \phi_k(x, y), \quad \phi_k(x, y) \text{ a solution of homogeneous PDE}$$

- analytical (only for specific forcing functions  $p(x, y, t)$  and boundary conditions), e.g., by separation of variables.

# Deformable mirrors — modeling

Static approximations: influence functions

$$w(x, y) = \sum_k^n h(x, y, s_k, t_k) u_k$$

- Cubic influence function:

$$h(x, y, s, t) = A(1 - 3(x - s)^2 + 2(x - s)^3)(1 - 3(y - t)^2 + 2(y - t)^3)$$

- Gaussian influence function:

$$h(x, y, s, t) = Ae^{r^2/\sigma^2}, \quad r = \sqrt{(x - s)^2 + (y - t)^2}$$

- Circular clamped edge faceplate<sup>1</sup> (polar coordinates):

$$h(r, \phi, \rho, \psi) = A(1 - r^2)(1 - \rho^2)(r^2 + \rho^2 - 2r\rho \cos(\phi - \psi)) \\ \times \ln \frac{r^2 + \rho^2 - 2r\rho \cos(\phi - \psi)}{1 + r^2\rho^2 - 2r\rho \cos(\phi - \psi)}$$

---

<sup>1</sup>Loktev et al., Comparison study of the performance of piston, thin plate and membrane mirrors for correction of turbulence-induced phase distortions, Optics Communications 192, 2001

# Deformable mirrors — modeling

Static approximations: influence functions

$$w(x, y) = \sum_k^n h(x, y, s_k, t_k) u_k$$

- Cubic influence function:

$$h(x, y, s, t) = A(1 - 3(x - s)^2 + 2(x - s)^3)(1 - 3(y - t)^2 + 2(y - t)^3)$$

- Gaussian influence function:

$$h(x, y, s, t) = Ae^{r^2/\sigma^2}, \quad r = \sqrt{(x - s)^2 + (y - t)^2}$$

- Circular clamped edge faceplate<sup>1</sup> (polar coordinates):

$$h(r, \phi, \rho, \psi) = A(1 - r^2)(1 - \rho^2)(r^2 + \rho^2 - 2r\rho \cos(\phi - \psi)) \\ \times \ln \frac{r^2 + \rho^2 - 2r\rho \cos(\phi - \psi)}{1 + r^2\rho^2 - 2r\rho \cos(\phi - \psi)}$$

---

<sup>1</sup>Loktev et al., Comparison study of the performance of piston, thin plate and membrane mirrors for correction of turbulence-induced phase distortions, Optics Communications 192, 2001

# Deformable mirrors — modeling

Static approximations: influence functions

$$w(x, y) = \sum_k^n h(x, y, s_k, t_k) u_k$$

- Cubic influence function:

$$h(x, y, s, t) = A(1 - 3(x - s)^2 + 2(x - s)^3)(1 - 3(y - t)^2 + 2(y - t)^3)$$

- Gaussian influence function:

$$h(x, y, s, t) = Ae^{r^2/\sigma^2}, \quad r = \sqrt{(x - s)^2 + (y - t)^2}$$

- Circular clamped edge faceplate<sup>1</sup> (polar coordinates):

$$h(r, \phi, \rho, \psi) = A(1 - r^2)(1 - \rho^2)(r^2 + \rho^2 - 2r\rho \cos(\phi - \psi)) \\ \times \ln \frac{r^2 + \rho^2 - 2r\rho \cos(\phi - \psi)}{1 + r^2\rho^2 - 2r\rho \cos(\phi - \psi)}$$

---

<sup>1</sup>Loktev et al., Comparison study of the performance of piston, thin plate and membrane mirrors for correction of turbulence-induced phase distortions, Optics Communications 192, 2001

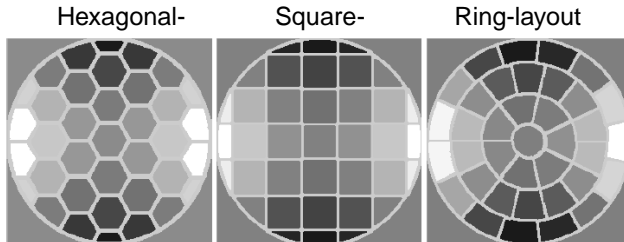
# Deformable mirrors — modeling

(Continued)

- Supported edge faceplate (c.f. Loktev et al., 2001)
- Free edge faceplate (idem)

# Deformable mirrors — modeling

Loktev et al. 2001, various actuator configurations and plate models are compared:



# Deformable mirrors — modeling

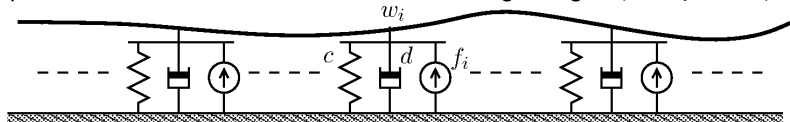
Residual wavefront aberrations for various type of mirrors each with 37 actuators (Credit: Loktev et al, 2001, Table 1 (adjusted))

Type of corrector	Error (%)	$B$ (rad <sup>2</sup> )	$N_{KL}$
<i>(a) Hexagonal structure</i>			
Piston	22.70	0.05282	5
Membrane	9.682	0.00961	29
Continuous faceplate, clamped edge	9.333	0.00892	31
Continuous faceplate, supported edge	9.306	0.00888	32
Continuous faceplate, free edge	9.022	0.00834	33
<i>(b) Ring segments</i>			
Piston	22.55	0.05214	6
Membrane	9.468	0.00918	31
Continuous faceplate, clamped edge	9.267	0.00880	32
Continuous faceplate, supported edge	9.238	0.00874	32
Continuous faceplate, free edge	9.107	0.00850	33
<i>(c) Squares</i>			
Piston	24.26	0.06031	4
Membrane	9.696	0.00963	29
Continuous faceplate, clamped edge	9.351	0.00895	31
Continuous faceplate, supported edge	9.321	0.00890	31
Continuous faceplate, free edge	9.119	0.00852	33



# Deformable mirrors — modeling

Example: finite difference discretization over hexagonal grid (Fraanje, 2010)



Thin plate model:

$$\left( E \nabla^4 \left( 1 + \eta \frac{\partial}{\partial t} \right) + \rho h \frac{\partial^2}{\partial t^2} \right) w(x, y, t) = p(x, y, t)$$

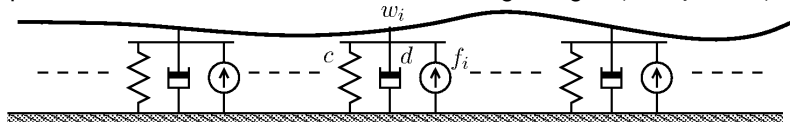
Actuator model at location  $(i, j)$ :

$$p(x_i, y_i, t) = \frac{1}{A} \left( f(i, j, t) - \underbrace{c \left( 1 + \zeta \frac{\partial}{\partial t} \right) w(x_i, y_i, t)}_{\text{spring/damper parallel to force}} \right)$$

Surface area of one hexagon  $A = \frac{3\sqrt{3}}{8} \Delta^2$ , where  $\Delta$  distance between two neighboring actuators.

# Deformable mirrors — modeling

Example: finite difference discretization over hexagonal grid (Fraanje, 2010)



Thin plate model:

$$\left( E \nabla^4 \left( 1 + \eta \frac{\partial}{\partial t} \right) + \rho h \frac{\partial^2}{\partial t^2} \right) w(x, y, t) = p(x, y, t)$$

Actuator model at location  $(i, j)$ :

$$p(x_i, y_i, t) = \frac{1}{A} \left( f(i, j, t) - \underbrace{c \left( 1 + \zeta \frac{\partial}{\partial t} \right) w(x_i, y_i, t)}_{\text{spring/damper parallel to force}} \right)$$

Surface area of one hexagon  $A = \frac{3\sqrt{3}}{8} \Delta^2$ , where  $\Delta$  distance between two neighboring actuators.

# Deformable mirrors — modeling

Discretization of biharmonic operator  $\nabla^4$  over hexagonal grid:

$$\begin{aligned}\mathcal{G}(S_1, S_2) = & \frac{4}{9} \left( 42 - 10(S_1 + S_1^{-1} + S_1 S_2^{-1} + S_1^{-1} S_2 + S_2 + S_2^{-1}) + \right. \\ & 2(S_1^2 S_2^{-1} + S_1^{-2} S_2 + S_1 S_2 + S_1^{-1} S_2^{-1} + S_1 S_2^{-2} + S_1^{-1} S_2^2) + \\ & \left. (S_1^2 + S_1^{-2} + S_1^2 S_2^{-2} + S_1^{-2} S_2^2 + S_2^2 + S_2^{-2}) \right)\end{aligned}$$

where  $S_1$  and  $S_2$  unit-shifts along principal axes of hexagonal grid.

Then PDE will reduce to interconnected ODE's:

$$\left( \frac{AEI}{\Delta^4} \mathcal{G}(S_1, S_2) \left( 1 + \eta \frac{\partial}{\partial t} \right) + c \left( 1 + \zeta \frac{\partial}{\partial t} \right) + \rho A h \frac{\partial^2}{\partial t^2} \right) w(i, j, t) = f(i, j, t)$$

(Note:  $I = h^3/12$  for thin plates.)

# Deformable mirrors — modeling

Discretization of biharmonic operator  $\nabla^4$  over hexagonal grid:

$$\begin{aligned}\mathcal{G}(S_1, S_2) = & \frac{4}{9} \left( 42 - 10(S_1 + S_1^{-1} + S_1 S_2^{-1} + S_1^{-1} S_2 + S_2 + S_2^{-1}) + \right. \\ & 2(S_1^2 S_2^{-1} + S_1^{-2} S_2 + S_1 S_2 + S_1^{-1} S_2^{-1} + S_1 S_2^{-2} + S_1^{-1} S_2^2) + \\ & \left. (S_1^2 + S_1^{-2} + S_1^2 S_2^{-2} + S_1^{-2} S_2^2 + S_2^2 + S_2^{-2}) \right)\end{aligned}$$

where  $S_1$  and  $S_2$  unit-shifts along principal axes of hexagonal grid.

Then PDE will reduce to interconnected ODE's:

$$\left( \frac{AEI}{\Delta^4} \mathcal{G}(S_1, S_2) \left( 1 + \eta \frac{\partial}{\partial t} \right) + c \left( 1 + \zeta \frac{\partial}{\partial t} \right) + \rho A h \frac{\partial^2}{\partial t^2} \right) w(i, j, t) = f(i, j, t)$$

(Note:  $I = h^3/12$  for thin plates.)

# Deformable mirrors — modeling

Let  $\dot{w} = \partial w / \partial t$  and  $\ddot{w} = \partial^2 w / \partial t^2$ , then

$$\begin{bmatrix} \dot{w}(i, j, t) \\ \ddot{w}(i, j, t) \end{bmatrix} = \begin{bmatrix} 0 \\ -\left(\frac{Eh^2 \mathcal{G}(S_1, S_2)}{12\rho\Delta^4} + \frac{8c}{3\sqrt{3}\rho\Delta^2 h}\right) \end{bmatrix} - \begin{bmatrix} 1 \\ \left(\frac{\eta Eh^2 \mathcal{G}(S_1, S_2)}{12\rho\Delta^4} + \frac{8\zeta c}{3\sqrt{3}\rho\Delta^2 h}\right) \end{bmatrix} \begin{bmatrix} w(i, j, t) \\ \dot{w}(i, j, t) \end{bmatrix} + \begin{bmatrix} 0 \\ \frac{8}{3\sqrt{3}\rho\Delta^2 h} \end{bmatrix} f(i, j, t)$$
$$w(i, j, t) = \begin{bmatrix} 1 & 0 \end{bmatrix} \begin{bmatrix} w(i, j, t) \\ \dot{w}(i, j, t) \end{bmatrix}$$

Stacking over all  $N$  nodes  $(i, j)$  yields:

$$\begin{aligned} \dot{x}(t) &= (I_N \otimes A_{a,c} + \mathcal{P}_N \otimes A_{b,c})x(t) + (I_N \otimes B_{a,c})f(t) \\ w(t) &= (I_N \otimes C_{a,c})x(t) \end{aligned}$$

where  $\mathcal{P}_N$  a sparse *pattern* matrix and ...

# Deformable mirrors — modeling

Let  $\dot{w} = \partial w / \partial t$  and  $\ddot{w} = \partial^2 w / \partial t^2$ , then

$$\begin{bmatrix} \dot{w}(i, j, t) \\ \ddot{w}(i, j, t) \end{bmatrix} = \begin{bmatrix} 0 \\ -\left(\frac{Eh^2 \mathcal{G}(S_1, S_2)}{12\rho\Delta^4} + \frac{8c}{3\sqrt{3}\rho\Delta^2 h}\right) \end{bmatrix} - \begin{bmatrix} 1 \\ \left(\frac{\eta Eh^2 \mathcal{G}(S_1, S_2)}{12\rho\Delta^4} + \frac{8\zeta c}{3\sqrt{3}\rho\Delta^2 h}\right) \end{bmatrix} \begin{bmatrix} w(i, j, t) \\ \dot{w}(i, j, t) \end{bmatrix} + \begin{bmatrix} 0 \\ \frac{8}{3\sqrt{3}\rho\Delta^2 h} \end{bmatrix} f(i, j, t)$$
$$w(i, j, t) = \begin{bmatrix} 1 & 0 \end{bmatrix} \begin{bmatrix} w(i, j, t) \\ \dot{w}(i, j, t) \end{bmatrix}$$

Stacking over all  $N$  nodes  $(i, j)$  yields:

$$\begin{aligned} \dot{x}(t) &= (I_N \otimes A_{a,c} + \mathcal{P}_N \otimes A_{b,c})x(t) + (I_N \otimes B_{a,c})f(t) \\ w(t) &= (I_N \otimes C_{a,c})x(t) \end{aligned}$$

where  $\mathcal{P}_N$  a sparse *pattern* matrix and ...

# Deformable mirrors — modeling

Stacking over all  $N$  nodes  $(i, j)$  yields:

$$\begin{aligned}\dot{x}(t) &= (I_N \otimes A_{a,c} + \mathcal{P}_N \otimes A_{b,c})x(t) + (I_N \otimes B_{a,c})f(t) \\ w(t) &= (I_N \otimes C_{a,c})x(t)\end{aligned}$$

where  $\mathcal{P}_N$  a sparse *pattern* matrix and

$$\begin{aligned}A_{a,c} &= \begin{bmatrix} 0 & 1 \\ -\frac{c}{m} & -\frac{\zeta c}{m} \end{bmatrix} & A_{b,c} &= \begin{bmatrix} 0 & 0 \\ -\frac{Eh^2}{12\rho\Delta^4} & -\frac{\eta Eh^2}{12\rho\Delta^4} \end{bmatrix} \\ B_{a,c} &= \begin{bmatrix} 0 & \frac{1}{m} \end{bmatrix}^T & C_{a,c} &= \begin{bmatrix} 1 & 0 \end{bmatrix}\end{aligned}$$

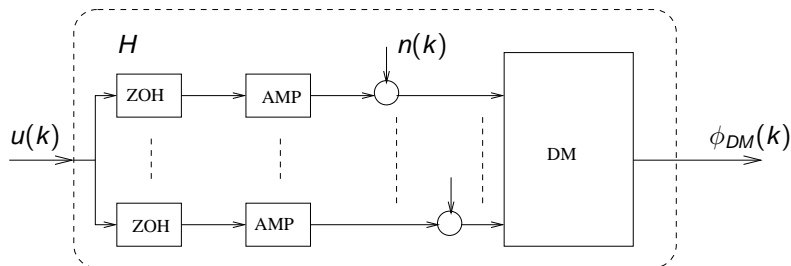
where  $m = \rho h \frac{3\sqrt{3}}{8} \Delta^2$  the mass of one hexagon.

# Deformable mirrors — modeling



# Deformable mirrors — modeling

# Control of AO systems

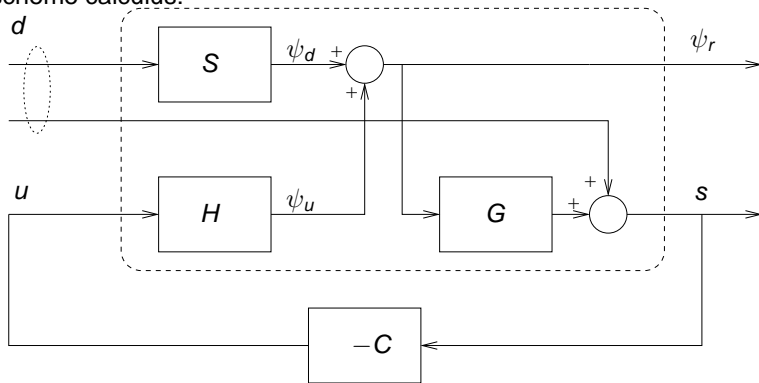


$$\phi_{DM}(k) = H_{DM} (L_{AMP} u(k) + n(k))$$

- Bandwidth of amplifiers;
- Noise-level of amplifiers;
- Dynamics of deformable mirror.

# Control of AO systems

Blockscheme calculus:



$$\begin{bmatrix} \psi_r \\ s \end{bmatrix} = \begin{bmatrix} S & H \\ GS & GH \end{bmatrix} \begin{bmatrix} d \\ u \end{bmatrix}$$
$$u = -Cs$$

Solve for  $\psi_r$

# Control of AO systems

$$\begin{bmatrix} \psi_r \\ s \end{bmatrix} = \begin{bmatrix} S & H \\ GS & GH \end{bmatrix} \begin{bmatrix} d \\ u \end{bmatrix}$$
$$u = -Cs$$

Solving for  $\psi_r$  yields:

$$\begin{aligned} u &= -CG\psi_r \\ &\iff \\ \psi_r &= Sd - HCG\psi_r \\ &\iff \\ (I + HCG)\psi_r &= Sd \\ &\iff \\ \psi_r &= (I + HCG)^{-1}Sd \end{aligned}$$

# Control of AO systems

$$\begin{bmatrix} \psi_r \\ s \end{bmatrix} = \begin{bmatrix} S & H \\ GS & GH \end{bmatrix} \begin{bmatrix} d \\ u \end{bmatrix}$$
$$u = -Cs$$

Solving for  $\psi_r$  yields:

$$\begin{aligned} u &= -CG\psi_r \\ &\iff \\ \psi_r &= Sd - HCG\psi_r \\ &\iff \\ (I + HCG)\psi_r &= Sd \\ &\iff \\ \psi_r &= (I + HCG)^{-1}Sd \end{aligned}$$

# Control of AO systems

Closed-loop residual wavefront phase:

$$\psi_r = (I + HCG)^{-1} Sd$$

Objective: minimize  $\|\psi_r\|_2^2$

How to design C?

$$|C| \rightarrow \infty \Rightarrow \|\psi_r\|_2^2 \rightarrow 0$$

High-gain feedback.

But, ...  $(I + HCG)^{-1}$  need to be stable!

# Control of AO systems

Closed-loop residual wavefront phase:

$$\psi_r = (I + HCG)^{-1} Sd$$

Objective: minimize  $\| \psi_r \|_2^2$

How to design C?

$$|C| \rightarrow \infty \Rightarrow \| \psi_r \|_2^2 \rightarrow 0$$

High-gain feedback.

But, ...  $(I + HCG)^{-1}$  need to be stable!

# Control of AO systems

Closed-loop residual wavefront phase:

$$\psi_r = (I + HCG)^{-1} Sd$$

Objective: minimize  $\| \psi_r \|_2^2$

How to design  $C$ ?

$$|C| \rightarrow \infty \Rightarrow \| \psi_r \|_2^2 \rightarrow 0$$

High-gain feedback.

But, ...  $(I + HCG)^{-1}$  need to be stable!



# Control of AO systems

Example:  $C = c$ ,  $H = az^{-1}$ ,  $G = S = 1$ , such that

$$\psi_r(k) = d(k) + au(k-1)$$

$$u(k) = -c\psi_r(k)$$

Closed-loop system:

$$\psi_r(k) = d(k) - ac\psi_r(k-1)$$

which is stable if and only if  $|ac| < 1, \rightarrow |c| < \frac{1}{|a|}$ .

# Control of AO systems

Example:  $C = c$ ,  $H = az^{-1}$ ,  $G = S = 1$ , such that

$$\psi_r(k) = d(k) + au(k-1)$$

$$u(k) = -c\psi_r(k)$$

Closed-loop system:

$$\psi_r(k) = d(k) - ac\psi_r(k-1)$$

which is stable if and only if  $|ac| < 1, \rightarrow |c| < \frac{1}{|a|}$ .

# Control of AO systems

Example:  $C = c$ ,  $H = az^{-1}$ ,  $G = S = 1$ , such that

$$\psi_r(k) = d(k) + au(k-1)$$

$$u(k) = -c\psi_r(k)$$

Closed-loop system:

$$\psi_r(k) = d(k) - ac\psi_r(k-1)$$

which is stable if and only if  $|ac| < 1, \rightarrow |c| < \frac{1}{|a|}$ .

# Control of AO systems

- 1 PID for MIMO systems;
- 2  $H_2$  optimal control;
- 3 Distributed control.

# Control: PID for MIMO systems

Control system:

$$\begin{aligned}s(k) &= G\psi_d(k) + \underbrace{GH}_{=P} u(k) \\ u(k+1) &= -C(z)s(k)\end{aligned}$$

Design strategy:

- Diagonalize system using SVD of  $P = U\Sigma V^T$ ;
- Design SISO controller.

Decoupled system:

$$\begin{aligned}s'(k) &= U^T G\psi_d(k) + \Sigma u'(k) \\ u'(k+1) &= -C'(z)s'(k)\end{aligned}$$

where  $s'(k) = U^T s(k)$ ,  $u'(k) = V^T u(k)$  and  $C(z) = VC'(z)U^T$ .  
 $C'(z)$  is designed as diagonal PI controller.

# Control: PID for MIMO systems

Control system:

$$\begin{aligned}s(k) &= G\psi_d(k) + \underbrace{GH}_{=P} u(k) \\ u(k+1) &= -C(z)s(k)\end{aligned}$$

Design strategy:

- Diagonalize system using SVD of  $P = U\Sigma V^T$ ;
- Design SISO controller.

Decoupled system:

$$\begin{aligned}s'(k) &= U^T G\psi_d(k) + \Sigma u'(k) \\ u'(k+1) &= -C'(z)s'(k)\end{aligned}$$

where  $s'(k) = U^T s(k)$ ,  $u'(k) = V^T u(k)$  and  $C(z) = VC'(z)U^T$ .  
 $C'(z)$  is designed as diagonal PI controller.

# Control: PID for MIMO systems

Control system:

$$\begin{aligned}s(k) &= G\psi_d(k) + \underbrace{GH}_{=P} u(k) \\ u(k+1) &= -C(z)s(k)\end{aligned}$$

Design strategy:

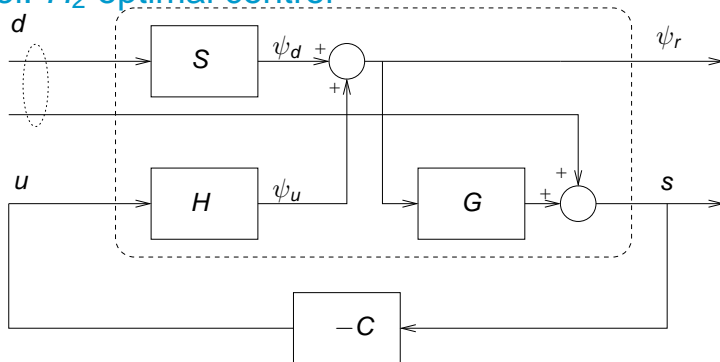
- Diagonalize system using SVD of  $P = U\Sigma V^T$ ;
- Design SISO controller.

Decoupled system:

$$\begin{aligned}s'(k) &= U^T G\psi_d(k) + \Sigma u'(k) \\ u'(k+1) &= -C'(z)s'(k)\end{aligned}$$

where  $s'(k) = U^T s(k)$ ,  $u'(k) = V^T u(k)$  and  $C(z) = VC'(z)U^T$ .  
 $C'(z)$  is designed as diagonal PI controller.

# Control: $H_2$ optimal control



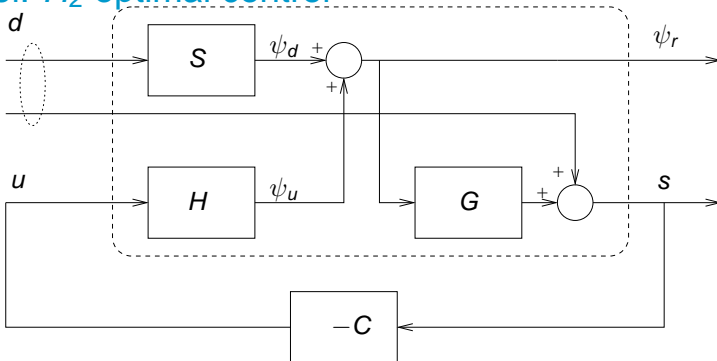
One “big” state-space model:

$$\begin{aligned} x(k+1) &= Ax(k) + Bu(k) + B_d d(k) \\ \psi_r(k) &= C_\psi x(k) + D_{\psi,u} u(k) + D_{\psi,d} d(k) \\ s(k) &= C_s x(k) + D_{s,d} d(k) \end{aligned}$$

Minimize transfer from  $d(k)$  to  $\psi_r(k)$ :  $\text{MSE}(\psi_r)/\text{MSE}(d)$



## Control: $H_2$ optimal control

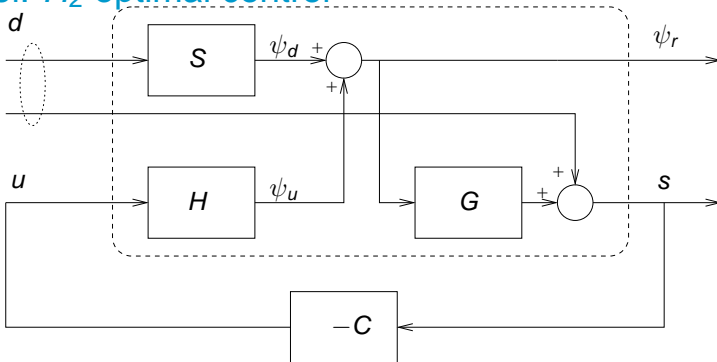


One “big” state-space model:

$$\begin{aligned}x(k+1) &= Ax(k) + Bu(k) + B_d d(k) \\ \psi_r(k) &= C_\psi x(k) + D_{\psi,u} u(k) + D_{\psi,d} d(k) \\ s(k) &= C_s x(k) + D_{s,d} d(k)\end{aligned}$$

Minimize transfer from  $d(k)$  to  $\psi_r(k)$ :  $\text{MSE}(\psi_r)/\text{MSE}(d)$

## Control: $H_2$ optimal control



One “big” state-space model:

$$\begin{aligned} x(k+1) &= Ax(k) + Bu(k) + B_d d(k) \\ \psi_r(k) &= C_\psi x(k) + D_{\psi,u} u(k) + D_{\psi,d} d(k) \\ s(k) &= C_s x(k) + D_{s,d} d(k) \end{aligned}$$

Minimize transfer from  $d(k)$  to  $\psi_r(k)$ :  $\text{MSE}(\psi_r)/\text{MSE}(d)$

# Control: $H_2$ optimal control

Solution:

- Kalman filter:

$$\begin{aligned}\hat{s}(k) &= C_s \hat{x}(k) \\ \hat{x}(k+1) &= A \hat{x}(k) + Bu(k) + K(s(k) - \hat{s}(k))\end{aligned}$$

where  $K$  the Kalman gain.

- State-feedback:

$$u(k+1) = -F \hat{x}(k+1)$$

where  $F$  the state-feedback gain.

For static deformable mirrors  $\psi_{DM}(k) = Hu(k)^2$ :

- Controller based on predicted wavefront:

$$u(k+1) = -H^\dagger \hat{\psi}(k+1)$$

where  $H$  the Moore-Penrose pseudo-inverse and  $\hat{\psi}(k+1) = C_\psi \hat{x}(k+1)$

---

<sup>2</sup>c.f., Hinnen, Data-Driven Optimal Control for Adaptive Optics, 2007, page 110

# Control: $H_2$ optimal control

Solution:

- Kalman filter:

$$\begin{aligned}\hat{s}(k) &= C_s \hat{x}(k) \\ \hat{x}(k+1) &= A \hat{x}(k) + Bu(k) + K(s(k) - \hat{s}(k))\end{aligned}$$

where  $K$  the Kalman gain.

- State-feedback:

$$u(k+1) = -F \hat{x}(k+1)$$

where  $F$  the state-feedback gain.

For static deformable mirrors  $\psi_{DM}(k) = Hu(k)^2$ :

- Controller based on predicted wavefront:

$$u(k+1) = -H^\dagger \hat{\psi}(k+1)$$

where  $H$  the Moore-Penrose pseudo-inverse and  $\hat{\psi}(k+1) = C_\psi \hat{x}(k+1)$

<sup>2</sup>c.f., Hinnen, Data-Driven Optimal Control for Adaptive Optics, 2007, page 110

# Control: $H_2$ optimal control

Solution:

- Kalman filter:

$$\begin{aligned}\hat{s}(k) &= C_s \hat{x}(k) \\ \hat{x}(k+1) &= A \hat{x}(k) + Bu(k) + K(s(k) - \hat{s}(k))\end{aligned}$$

where  $K$  the Kalman gain.

- State-feedback:

$$u(k+1) = -F \hat{x}(k+1)$$

where  $F$  the state-feedback gain.

For static deformable mirrors  $\psi_{DM}(k) = Hu(k)^2$ :

- Controller based on predicted wavefront:

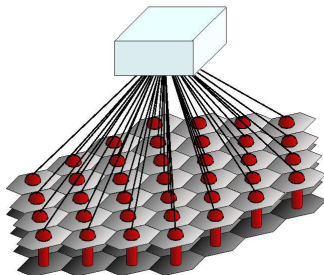
$$u(k+1) = -H^\dagger \hat{\psi}(k+1)$$

where  $H$  the Moore-Penrose pseudo-inverse and  $\hat{\psi}(k+1) = C_\psi \hat{x}(k+1)$

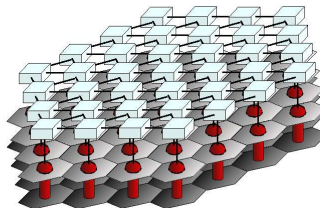
<sup>2</sup>c.f., Hinnen, Data-Driven Optimal Control for Adaptive Optics, 2007, page 110

# Control: Distributed control

(Fraanje, Massioni, Verhaegen 2011)  
centralized controller

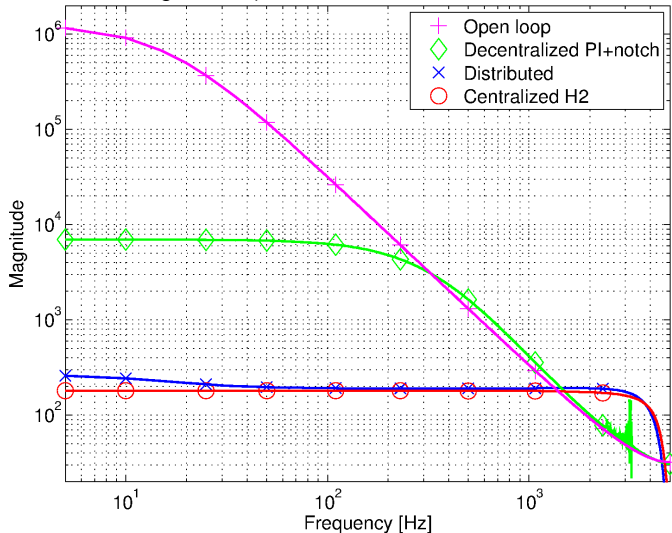


distributed controllers



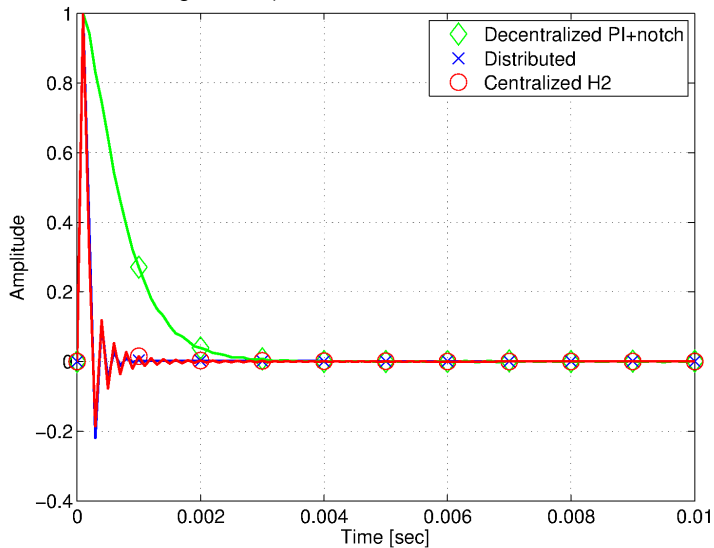
# Control: Distributed control

(Fraanje, Massioni, Verhaegen 2011)



# Control: Distributed control

(Fraanje, Massioni, Verhaegen 2011)





# Exams

- 1 Sparse matrix techniques for wavefront reconstruction;
- 2 Extended object and wavefront estimation by phase-diversity;
- 3 Pyramide wavefront sensor;
- 4 Adaptive optics for the eye;
- 5 Quantum noise effects in imaging;
- 6 Data-driven  $H_2$  control;
- 7 Modeling and validation of deformable mirrors.

# Exams

- 1 Sparse matrix techniques for wavefront reconstruction;
- 2 Extended object and wavefront estimation by phase-diversity;
- 3 Pyramide wavefront sensor;
- 4 Adaptive optics for the eye;
- 5 Quantum noise effects in imaging;
- 6 Data-driven  $H_2$  control;
- 7 Modeling and validation of deformable mirrors.

# Exams

- 1 Sparse matrix techniques for wavefront reconstruction;
- 2 Extended object and wavefront estimation by phase-diversity;
- 3 Pyramide wavefront sensor;
- 4 Adaptive optics for the eye;
- 5 Quantum noise effects in imaging;
- 6 Data-driven  $H_2$  control;
- 7 Modeling and validation of deformable mirrors.

# Exams

- 1 Sparse matrix techniques for wavefront reconstruction;
- 2 Extended object and wavefront estimation by phase-diversity;
- 3 Pyramide wavefront sensor;
- 4 Adaptive optics for the eye;
- 5 Quantum noise effects in imaging;
- 6 Data-driven  $H_2$  control;
- 7 Modeling and validation of deformable mirrors.

# Exams

- 1 Sparse matrix techniques for wavefront reconstruction;
- 2 Extended object and wavefront estimation by phase-diversity;
- 3 Pyramide wavefront sensor;
- 4 Adaptive optics for the eye;
- 5 Quantum noise effects in imaging;
- 6 Data-driven  $H_2$  control;
- 7 Modeling and validation of deformable mirrors.

# Exams

- 1 Sparse matrix techniques for wavefront reconstruction;
- 2 Extended object and wavefront estimation by phase-diversity;
- 3 Pyramide wavefront sensor;
- 4 Adaptive optics for the eye;
- 5 Quantum noise effects in imaging;
- 6 Data-driven  $H_2$  control;
- 7 Modeling and validation of deformable mirrors.

# Exams

- 1 Sparse matrix techniques for wavefront reconstruction;
- 2 Extended object and wavefront estimation by phase-diversity;
- 3 Pyramide wavefront sensor;
- 4 Adaptive optics for the eye;
- 5 Quantum noise effects in imaging;
- 6 Data-driven  $H_2$  control;
- 7 Modeling and validation of deformable mirrors.